# X-ray diffraction analysis of a human tRNA^Gly acceptor-stem microhelix isoacceptor at 1.18 Å resolution

**André Eichert,[a] Markus Perbandt,[b] Angela Schreiber,[a] Jens P. Fürste,[a] Christian Betzel,[c] Volker A. Erdmann[a] and Charlotte Förster[a]\***

[a]Institute of Chemistry and Biochemistry, Free University Berlin, Thielallee 63, 14195 Berlin, Germany, [b]Institute of Biochemistry, Laboratory for Structural Biology of Infection and Inflammation, University of Lübeck, Building 22a, c/o DESY, 22603 Hamburg, Germany, and [c]Institute of Biochemistry and Food Chemistry, University of Hamburg, Notkestrasse 85, Building 22a, c/o DESY, 22603 Hamburg, Germany

Correspondence e-mail: foerster@chemie.fu-berlin.de

Interest has been focused on comparative X-ray structure analyses of different tRNA^Gly acceptor-stem helices. tRNA^Gly/glycyl-tRNA synthetase belongs to the so-called class II system, in which the tRNA identity elements consist of simple and unique determinants that are located in the tRNA acceptor stem and the discriminator base. Comparative structure investigations of tRNA^Gly micro-helices provide insight into the role of tRNA identity elements. Predominant differences in the structures of glycyl-tRNA synthetases and in the tRNA identity elements between prokaryotes and eukaryotes point to divergence during the evolutionary process. Here, the crystallization and high-resolution X-ray diffraction analysis of a human tRNA^Gly acceptor-stem microhelix with sequence $5'$-$G_1C_2A_3U_4U_5G_6G_7$-$3'$, $5'$-$C_{66}C_{67}A_{68}A_{69}U_{70}G_{71}C_{72}$-$3'$ is reported. The crystals belonged to the monoclinic space group $C2$, with unit-cell parameters $a = 37.32$, $b = 37.61$, $c = 30.47$ Å, $\beta = 112.60°$ and one molecule per asymmetric unit. A data set was collected using synchrotron radiation and data were processed within the resolution range 50.0–1.18 Å. The structure was solved by molecular replacement.

## 1. Introduction

tRNA identity elements assure the aminoacylation of tRNA by the cognate aminoacyl-tRNA synthetases. Owing to the redundancy of the genetic code, there are several isoacceptor tRNAs which code for the same amino acid but recognize different codons on the messenger RNA. Identity elements which consist of structure and/or sequence motifs on the tRNA determine the correct aminoacylation of tRNA isoacceptors and avoid the misaminoacylation of noncognate tRNAs.

Two different groups of tRNA/aminoacyl-tRNA synthetase systems exist. Class I tRNA/aminoacyl-tRNA synthetases possess complex identity elements which are mostly spread over different parts of the tRNA including the anticodon (Eriani *et al.*, 1990). Within the class II system, tRNA identity elements consist of a small number of simple determinants (Eriani *et al.*, 1990). These are located in the aminoacyl stem and sometimes include the discriminator base at position 73 of the tRNA. Such tRNA determinants can be so simple as to consist of only one base pair. This has been shown for the *Escherichia coli* tRNA^Ala (Hou & Schimmel, 1988).

tRNA^Gly/glycyl-tRNA synthetase (GlyRS) belongs to the class II system. In *E. coli*, the tRNA^Gly identity determinants consist of a conserved base pair C2·G71 and the U73 discriminator base (Mc-Clain *et al.*, 1991). Nevertheless, the glycine system is a special case within class II as there are large differences in the synthetase structure and the tRNA identity elements between eukaryotic/archae-bacterial and eubacterial organisms.

The eubacterial GlyRS has been well investigated. *E. coli* GlyRS, a tetrameric protein, consists of an $\alpha_2\beta_2$ structure; both subunits are required for activity (Ostrem & Berg, 1974; Webster *et al.*, 1983). The $\beta$-subunit is responsible for tRNA binding (Nagel *et al.*, 1984). Amino-acid activation, which involves the binding of ATP and

# crystallization communications
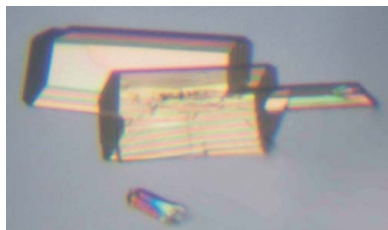
glycine, is governed by the $\alpha$-subunit (Toth & Schimmel, 1990a,b). The tRNA identity elements are located on the aminoacyl stem and include the discriminator base, which has to be uracil.

In contrast, the eukaryotic/archaebacterial GlyRS is a simpler enzyme consisting of an $\alpha_2$ structure (Kern et al., 1981; Nada et al., 1993; Shiba et al., 1994; Shiba, 2005). The tRNA identity elements also differ between prokaryotes and eukaryotes. A major difference in tRNA$^{Gly}$ identity is the discriminator base, which is strictly adenosine in the eukaryotic/archaebacterial case but is known to be uracil in the prokaryotic system (Shiba et al., 1994). In general, GlyRS also differs from most other class II aminoacyl-tRNA synthetases with respect to the three highly conserved binding motifs. The eukaryotic/archaebacterial system possesses three unique class II motifs 1–3, which all consist of a strongly conserved sequence. Motif 1 contains a G$\Phi$XX$\Phi$XXP$\Phi\Phi$ region, motif 2 a (F/Y/H)R$X$(E/D) stretch and motif 3 possesses a $\lambda X\Phi$G$\Phi$G$\Phi$ER$\Phi\Phi\Phi\Phi\Phi$ sequence (Eriani et al., 1990), in which $X$ represents any residue, $\Phi$ a hydrophobic residue and $\lambda$ a short-chain residue. The distance between motif 1 and motif 3 is relatively constant and lies between 40 and 80 residues, whereas the distance between motifs 2 and 3 can consist of between 70 and 300 residues (Eriani et al., 1990). In the prokaryotic enzymes only motif 3 is present; motifs 1 and 2 are possibly degenerated and could not be found in the primary sequences of the proteins (Moras, 1992; Shiba, 2005).

The glycine system becomes even more complicated when studying *Thermus thermophilus* GlyRS. The crystal structure of this enzyme has been solved to 2.75 Å resolution (Logan et al., 1995). The structure of the thermophilic GlyRS somewhat resembles the subunit arrangement of the eukaryotic/archaebacterial-type enzymes, whilst the tRNA identity elements show the features of the eubacterial tRNAs.

Here, we report the crystallization and high-resolution X-ray diffraction analysis of the human tRNA$^{Gly}$ acceptor stem at 1.18 Å resolution. The structure was solved by molecular replacement. Comparative structure analysis with other tRNA$^{Gly}$ acceptor-stem helices (Förster, Brauer et al., 2007; Förster et al., 2008) will help in understanding the tRNA$^{Gly}$–GlyRS system at the structural level in the region of the acceptor stem.

## 2. Materials and methods

### 2.1. Crystallization of the human tRNA$^{Gly}$ acceptor-stem microhelix isoacceptor DG9990
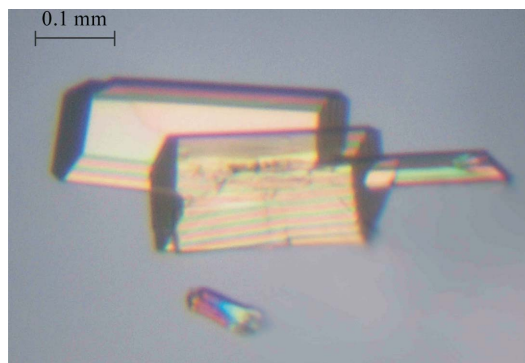
The human tRNA$^{Gly}$ acceptor-stem microhelix isoacceptor investigated here was derived from the gene sequence with tRNA Database ID DG9990 (Sprinzl & Vassilenko, 2005) and is the counterpart of the human tRNA$^{Gly}$ microhelix structure (derived from DG9992) that has recently been published (Förster et al., 2008). The oligonucleotides 5′-GCAUUGG-3′ and 5′-CCAAUGC-3′ which form the tRNA$^{Gly}$ (DG9990) microhelix were purchased from IBA (Göttingen, Germany) at HPLC purification grade. The exact concentration of the RNA single strands was determined by alkaline hydrolysis, considering the molar extinction coefficients of the single nucleotides and using UV spectroscopy as described in Sproat et al. (1995), and both strands were annealed in water at a concentration of 0.5 m$M$. For this procedure, the strands were combined and heated to 363 K for 5 min and then cooled to room temperature for several hours. The resulting tRNA$^{Gly}$ duplex was used in crystallization experiments without further purification.

We used two different nucleic acid crystal screening kits from Hampton Research (California, USA) for initial crystallization experiments. The Natrix Nucleic Acid Crystallization Kit (HR2-116; Hampton Research, California, USA) containing 48 different crystallization conditions was used with the sitting-drop vapour-diffusion technique and CrystalQuick Lp plates from Greiner Bio-One (Germany). 1 µl of the aqueous RNA solution at a concentration of 0.5 m$M$ was mixed with 1 µl reservoir solution and equilibrated against 80 µl reservoir solution at 294 K. In parallel, the Nucleic Acid Mini Screen (HR2-118; Hampton Research, California, USA) with 24 different conditions was used with the hanging-drop vapour-diffusion technique and Linbro plates (ICN Biomedicals Inc., Ohio, USA). In this screening procedure, 1 µl 0.5 m$M$ aqueous RNA solution was mixed with 1 µl crystallization solution from the screen and equilibrated against 1 ml reservoir solution consisting of 35%($v/v$) MPD (2-methyl-2,4-pentanediol) in water pH 7.4 at a temperature of 294 K. Many tiny crystals appeared after 1–2 d using different crystallization conditions with 35%($v/v$) MPD in the reservoirs. Only one condition yielded larger crystals with dimensions of approximately $0.3 \times 0.1 \times 0.1$ mm (Fig. 1). These crystals grew in 10%($v/v$) MPD, 40 m$M$ sodium cacodylate pH 6.0, 12 m$M$ spermine tetrachloride, 80 m$M$ potassium chloride with equilibration against 35%($v/v$) MPD at 294 K and appeared after 12 d. This condition was an initial crystallization solution from the Hampton screen and was not further optimized. Nevertheless, several crystallization setups were performed with this crystallization solution using the hanging-drop vapour-diffusion technique in Linbro plates and the best crystals were used for data collection.

### 2.2. Acquisition of X-ray diffraction data and data processing

Prior to X-ray diffraction data collection, the crystals were flash-frozen in liquid nitrogen. The crystallization buffer, which contained 10%($v/v$) MPD, was directly used for freezing without the addition of any further cryoprotectant solution. The X-ray diffraction data were recorded on Diamond Synchrotron beamline I04 (UK) at a wavelength of 0.9696 Å. A high-resolution data set was recorded from 50 to 1.18 Å at a temperature of 100 K. All data were analyzed and processed using programs from the *HKL*-2000 suite (Otwinowski & Minor, 1997). The data set of the tRNA$^{Gly}$ helix was analyzed for merohedral twinning using the Padilla and Yeates algorithm (Padilla & Yeates, 2003) as implemented in the web server http://nihserver.mbi.ucla.edu/pystats. The structure was solved by molecular replacement using the program *Phaser* (McCoy et al., 2005) with the human tRNA$^{Gly}$ acceptor-stem microhelix isoacceptor G9992 (PDB code 2v7r) as a search model (Förster et al., 2008). Structure



**Figure 1**
Crystals of the human tRNA$^{Gly}$ acceptor-stem microhelix isoacceptor derived from gene sequence DG9990 (Sprinzl & Vassilenko, 2005) with approximate dimensions of $0.30 \times 0.10 \times 0.10$ mm. The crystals were successfully separated before data collection.

refinement is in progress using the program *REFMAC*5 (Murshudov *et al.*, 1997). Both programs were used as implemented in the *CCP4i* package (Collaborative Computational Project, Number 4, 1994).

## 3. Results and discussion

### 3.1. Crystallization

For human cytoplasm, three of the four different sequences for tRNA$^{Gly}$ isoacceptor genes are available in the database of Sprinzl & Vassilenko (2005), with identification numbers DG9990, DG9991 and DG9992, of which DG9990 and DG9991 have identical sequences in their acceptor stems. The crystallization and the X-ray structure of the human tRNA$^{Gly}$ isoacceptor derived from gene sequence DG9992 have recently been published (Förster, Szkaradkiewicz *et al.*, 2007; Förster *et al.*, 2008). The two tRNA$^{Gly}$s DG9992 and DG9990 possess different anticodons, UCC and GCC, respectively, matching the mRNA triplets coding for glycine. Nevertheless, both tRNAs are aminoacylated with the same amino acid; we therefore focused on comparative structural analyses of the aminoacyl stems of these isoacceptors. We have now successfully crystallized the human cyto-plasmic tRNA$^{Gly}$ isoacceptor with the sequence 5′-G$_1$C$_2$A$_3$U$_4$-U$_5$G$_6$G$_7$-3′ and 5′-C$_{66}$C$_{67}$A$_{68}$A$_{69}$U$_{70}$G$_{71}$C$_{72}$-3′ (derived from gene sequence DG9990; Figs. 1 and 2). A high-resolution data set was recorded and X-ray diffraction data were processed in the 50–1.18 Å resolution range.

### 3.2. Crystallographic data

Like the recently described human tRNA$^{Gly}$ microhelix (DG9992; Förster, Szkaradkiewicz *et al.*, 2007), the human tRNA$^{Gly}$ acceptor-stem microhelix investigated here (DG9990) crystallized in space
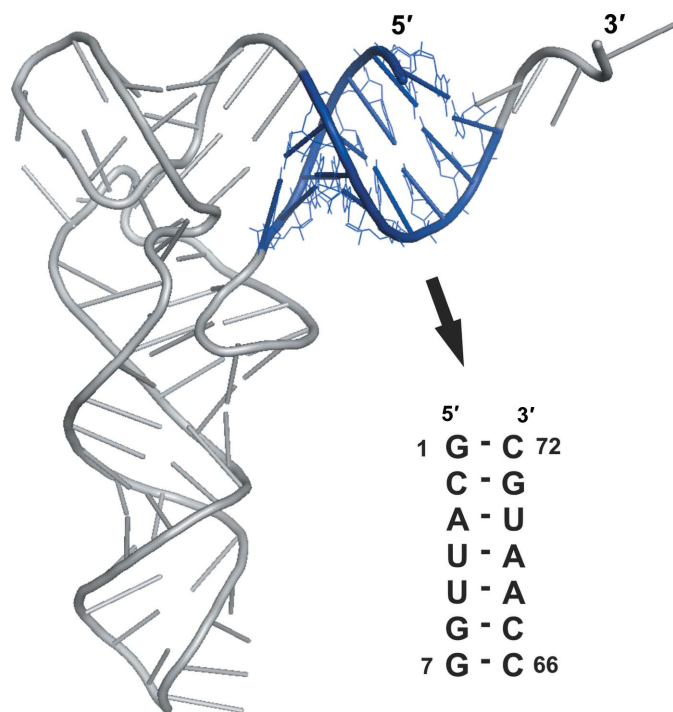


**Figure 2**
The tRNA secondary structure derived from yeast tRNA$^{Phe}$ (Shi & Moore, 2000). The aminoacyl stem region with the sequence of the human tRNA$^{Gly}$ microhelix analyzed in this study is pointed out by an arrow and indicated in blue in the structure. The ribbon represents the tRNA phosphodiester backbone; the batons represent ribose sugars and bases.

**Table 1**
Data-collection and processing statistics of the human cytoplasmatic tRNA$^{Gly}$ acceptor-stem microhelix isoacceptor derived from the gene sequence with tRNA Database ID DG9990 (Sprinzl & Vassilenko, 2005).

Values in parentheses are for the highest resolution shell.

| | |
|---|---|
| Beamline | Diamond, I04 |
| Wavelength (Å) | 0.9696 |
| Space group | *C*2 |
| Unit-cell parameters (Å, °) | *a* = 37.32, *b* = 37.61, *c* = 30.47, β = 112.60 |
| Matthews coefficient $V_M$† (Å$^3$ Da$^{-1}$) | 2.25 |
| RNA duplexes in asymmetric unit | 1 |
| Solvent content‡ (%) | 58.0 |
| Measured reflections | 133399 |
| Unique reflections | 12058 |
| Resolution range (Å) | 50.0–1.18 (1.22–1.18) |
| Completeness (%) | 93.5 (87.0) |
| Multiplicity | 11.1 (7.5) |
| $R_{merge}$§ (%) | 8.0 (21.3) |
| Average $I/\sigma(I)$ | 22.9 (1.8) |

† Matthews (1968). ‡ Estimated using the average partial specific volume calculated for RNA by Voss & Gerstein (2005). § $R_{merge} = \sum_{hkl} \sum_i |I_i(hkl) - \langle I(hkl)\rangle| / \sum_{hkl} \sum_i I_i(hkl)$, where $I_i(hkl)$ and $\langle I(hkl)\rangle$ are the observed individual and mean intensities of a reflection with indices *hkl*, respectively, $\sum_i$ is the sum over the individual measurements of a reflection with indices *hkl* and $\sum_{hkl}$ is the sum over all reflections.

group *C*2. A high-resolution data set was acquired using synchrotron radiation and cryogenic cooling on Diamond Synchrotron beamline I04 (UK).

The crystallographic parameters of the tRNA$^{Gly}$ acceptor-stem microhelix (DG9990) are listed in Table 1. The unit-cell parameters of the DG9990 tRNA$^{Gly}$ microhelix reported here are fairly similar to those of the previously published DG9992 (Förster, Szkaradkiewicz *et al.*, 2007).

A merohedral twinning analysis was applied to the crystallographic data using the Padilla and Yeates algorithm (Padilla & Yeates, 2003), since merohedral twinning can occur in crystals of short RNA duplexes (Rypniewski *et al.*, 2006; Mueller, Muller *et al.*, 1999; Mueller, Schübel *et al.*, 1999). Analysis of the tRNA$^{Gly}$ microhelix (DG9990) data set showed a curve which corresponds to a theore-tically untwinned crystal; there was no indication of merohedral twinning.

The structure of the human tRNA$^{Gly}$ microhelix was solved by molecular replacement using the program *Phaser* (McCoy *et al.*, 2005) with the coordinates of the human tRNA$^{Gly}$ microhelix isoacceptor with PDB code 2v7r (Förster *et al.*, 2008) as a search model. The initial *R* value after molecular replacement was 36.0%, with a correlation coefficient of 56.6 and *Z* scores of 10.1 in the rotation function and 10.9 in the translation function. The structure is presently being refined and the *R* and $R_{free}$ values were approxi-mately 20% and 23%, respectively, after adding solvent molecules (data not shown).

We will focus on comparative structure analysis between the human cytoplasmatic tRNA$^{Gly}$ microhelices reported here and published previously (Förster *et al.*, 2008). Additionally, the *E. coli* tRNA$^{Gly}$ microhelix X-ray structure (Förster, Brauer *et al.*, 2007) will be used for superposition experiments. The two human tRNA$^{Gly}$ microhelices crystallize without magnesium, whereas in the *E. coli* tRNA$^{Gly}$ microhelix a magnesium-binding site could be identified within the region of the tRNA identity elements (Förster, Brauer *et al.*, 2007). This magnesium-binding site has also been reported for *E. coli* tRNA$^{Ala}$ (Limmer *et al.*, 1993) and for yeast tRNA$^{Phe}$ (Shi & Moore, 2000). Soaking experiments with the human tRNA$^{Gly}$ micro-helix crystals are under way to investigate potential magnesium-binding sites. A detailed comparison of the water molecules bound to the human tRNA$^{Gly}$ microhelix structures will provide insight into the

hydration patterns. This is of importance for initial protein–RNA contacts, which we believe to be facilitated *via* bound solvent molecules. Our investigations support the structure–function relationship within the different tRNA[Gly] systems with respect to the evolutionary divergence between eubacteria and eukaryotes/archaebacteria.

## References

Collaborative Computational Project, Number 4 (1994). *Acta Cryst.* D**50**, 760–763.

Eriani, G., Delarue, M., Poch, O., Gangloff, J. & Moras, D. (1990). *Nature (London)*, **347**, 203–206.

Förster, C., Brauer, A. B. E., Perbandt, M., Lehmann, D., Fürste, J. P., Betzel, C. & Erdman, V. A. (2007). *Biochem. Biophys. Res. Commun.* **363**, 621–625.

Förster, C., Mankowska, M., Fürste, J. P., Perbandt, M., Betzel, C. & Erdmann, V. A. (2008). *Biochem. Biophys. Res. Commun.* **368**, 996–1001.

Förster, C., Szkaradkiewicz, K., Perbandt, M., Brauer, A. B. E., Borowski, T., Fürste, J. P., Betzel, C. & Erdmann, V. A. (2007). *Acta Cryst.* F**63**, 858–861.

Hou, Y. M. & Schimmel, P. (1988). *Nature (London)*, **333**, 140–145.

Kern, D., Giegé, R. & Ebel, J. P. (1981). *Biochemistry*, **20**, 122–131.

Limmer, S., Hofmann, H.-P., Ott, G. & Sprinzl, M. (1993). *Proc. Natl Acad. Sci. USA*, **90**, 6199–6202.

Matthews, B. W. (1968). *J. Mol. Biol.* **33**, 491–497.

McClain, W. H., Foss, K., Jenkins, R. A. & Schneider, J. (1991). *Proc. Natl Acad. Sci. USA*, **88**, 6147–6151.

McCoy, A. J., Grosse-Kunstleve, R. W., Storoni, L. C. & Read, R. J. (2005). *Acta Cryst.* D**61**, 458–464.

Moras, D. (1992). *Trends Biochem. Sci.* **17**, 159–164.

Mueller, U., Muller, Y. A., Herbst-Irmer, R., Sprinzl, M. & Heinemann, U. (1999). *Acta Cryst.* D**55**, 1405–1413.

Mueller, U., Schübel, H., Sprinzl, M. & Heinemann, U. (1999). *RNA*, **5**, 670–677.

Murshudov, G. N., Vagin, A. A. & Dodson, E. J. (1997). *Acta Cryst.* D**53**, 240–255.

Nada, S., Chang, P. K. & Dignam, J. D. (1993). *J. Biol. Chem.* **268**, 7660–7667.

Nagel, G. M., Cumberledge, S., Johnson, M. S., Petrella, E. & Weber, B. (1984). *Nucleic Acids Res.* **12**, 4377–4384.

Ostrem, D. L. & Berg, P. (1974). *Biochemistry*, **13**, 1338–1348.

Otwinowski, Z. & Minor, W. (1997). *Methods Enzymol.* **276**, 307–326.

Padilla, J. E. & Yeates, T. O. (2003). *Acta Cryst.* D**59**, 1124–1130.

Rypniewski, W., Vallazza, M., Perbandt, M., Klussmann, S., DeLucas, L. J., Betzel, C. & Erdmann, V. A. (2006). *Acta Cryst.* D**62**, 659–664.

Shi, H. & Moore, P. B. (2000). *RNA*, **6**, 1091–1105.

Shiba, K. (2005). *The Aminoacyl-tRNA Synthetases*, pp. 125–134. Georgetown, USA: Landes Bioscience.

Shiba, K., Schimmel, P., Motegi, H. & Noda, T. (1994). *J. Biol. Chem.* **269**, 30049–30055.

Sprinzl, M. & Vassilenko, K. S. (2005). *Nucleic Acids Res.* **33**, D139–D140.

Sproat, B., Colonna, F., Mullah, B., Tsou, D., Andrus, A., Hampel, A. & Vinayak, R. (1995). *Nucleosides Nucleotides*, **14**, 255–273.

Toth, M. J. & Schimmel, P. (1990a). *J. Biol. Chem.* **265**, 1000–1004.

Toth, M. J. & Schimmel, P. (1990b). *J. Biol. Chem.* **265**, 1005–1009.

Voss, N. R. & Gerstein, M. (2005). *J. Mol. Biol.* **346**, 477–492.

Webster, T. A., Gibson, B. W., Keng, T., Biemann, K. & Schimmel, P. (1983). *J. Biol. Chem.* **258**, 10637–10641.